

Differentially private sliced inverse regression in the federated paradigm

Shuaida He*, Jiarui Zhang[†], Xin Chen[‡]

June 09, 2023

Abstract

We extend the celebrated sliced inverse regression to address the challenges of decentralized data, prioritizing privacy and communication efficiency. Our approach, federated sliced inverse regression (FSIR), facilitates collaborative estimation of the sufficient dimension reduction subspace among multiple clients, solely sharing local estimates to protect sensitive datasets from exposure. To guard against potential adversary attacks, FSIR further employs diverse perturbation strategies, including a novel multivariate Gaussian mechanism that guarantees differential privacy at a low cost of statistical accuracy. Additionally, FSIR naturally incorporates a collaborative variable screening step, enabling effective handling of high-dimensional client data. Theoretical properties of FSIR are established for both low-dimensional and high-dimensional settings, supported by extensive numerical experiments and real data analysis.

1 Introduction

In recent years, preserving data ownership and privacy in statistical data analysis has gained significant importance. In numerous applications, records carrying sensitive personal information are sourced from diverse origins, posing challenges in aggregating them into a unified dataset for joint analysis. This obstacle arises from commonly known transmission restrictions, such as expensive communication costs between a central server and local sites, but it is the privacy concerns that greatly intensify it. A typical example highlighting this challenge is the collection of patient-level observations from different clinical sites (Duan et al., 2022; Tong et al., 2022; Liu et al., 2022).

To this end, efficiently extracting valid information from decentralized data while preserving data privacy is critical. Federated learning (McMahan et al., 2017; Li et al., 2020), a widely adopted distributed computing framework, has emerged as a promising approach that emphasizes privacy protection by aggregating partial estimates from different clients to yield a centralized model. However, while this computing paradigm preserves client data ownership, it does not directly guarantee record-level privacy, a crucial concern in scenarios lacking a trusted central server or a secure communication environment. In such cases, adversaries can access statistics calculated by local clients during the uploading procedure (Homer et al.,

*Department of Statistics and Data Science, Southern University of Science and Technology, Shenzhen, China.

[†]Co-first author. Department of Statistics and Data Science, Southern University of Science and Technology, Shenzhen, China.

[‡]Corresponding author. Department of Statistics and Data Science, Southern University of Science and Technology, Shenzhen 518055, China; Email: chenx8@sustech.edu.cn

2008; Calandrino et al., 2011), posing risks of various privacy attacks, including re-identification, reconstruction, and tracing attacks (Bun et al., 2014; Dwork et al., 2015; Kamath et al., 2019), among others.

The tracing attack, also known as membership inference attack, is particularly insidious among those adversaries, as it attempts to identify whether a target individual is a member of a given dataset. While this may appear as a subtle privacy breach, extensive research has demonstrated that even the presence of a single record in a specific dataset can be highly sensitive information (Dwork et al., 2017). This type of information is closely connected to the concept of differential privacy (Dwork et al., 2006), a rigorous definition of privacy widely adopted in both academia (Dwork and Lei, 2009; Wasserman and Zhou, 2010; Avella-Medina, 2021; Drechsler, 2022) and real-world applications (Erlingsson et al., 2014; Apple, 2017; Ding et al., 2017; Drechsler, 2023). To be specific, a randomized algorithm or mechanism $\mathcal{M} : \mathcal{X}^n \rightarrow \mathcal{T}$ guarantees (ϵ, δ) -differential privacy if

$$P(\mathcal{M}(\mathcal{D}) \in \mathcal{S}) \leq e^\epsilon P(\mathcal{M}(\mathcal{D}') \in \mathcal{S}) + \delta \quad (1)$$

for all measurable $\mathcal{S} \subseteq \mathcal{T}$ and all datasets $\mathcal{D}, \mathcal{D}' \in \mathcal{X}^n$ that differ in a single record. The parameter set (δ, ϵ) controls the level of privacy. Intuitively, $\mathcal{M}(\mathcal{D})$ captures the global characteristics of \mathcal{D} , and the goal of privacy is to simultaneously protect every record in \mathcal{D} while releasing $\mathcal{M}(\mathcal{D})$. A common strategy to construct a differentially private estimator is perturbing its non-private counterpart by random noises (Dwork et al., 2014). Along this line, a variety of fundamental data analyses, such as mean estimation (Kamath et al., 2019), covariance estimation (Biswas et al., 2020), linear regression (Talwar et al., 2015), have been revisited in the context of (ϵ, δ) -differential privacy protection. In particular, Cai et al. (2021) proposed a sharp tracing attack to establish minimax lower bounds for differentially private mean estimation and linear regression.

This paper proposes a federated computation framework for estimating the subspace pursued by a class of supervised dimension reduction methods, termed sufficient dimension reduction (SDR, (Cook, 1994)), with the guarantee of differential privacy. Briefly speaking, SDR seeks to replace the original predictors $X = (X_1, \dots, X_p)^\top$ in a regression problem with a minimal set of their linear combinations without loss of information for predicting the response Y . Mathematically, this can be expressed as

$$Y \perp\!\!\!\perp X | \beta^\top X, \quad (2)$$

where $\beta \in \mathbb{R}^{p \times d}$ ($d < p$) and $\perp\!\!\!\perp$ indicates independence. The subspace spanned by β , denoted by $\mathcal{S}_{Y|X} \triangleq \text{span}(\beta)$, is the parameter of interest and known as the sufficient dimension reduction subspace, or SDR subspace (Cook, 1996, 2009). Here $d = \dim(\mathcal{S}_{Y|X})$ is often called the structure dimension. To illustrate the potential risk of privacy breaches in estimating $\mathcal{S}_{Y|X}$, we provide a motivating example.

Example 1 (A tracing attack on linear discriminant analysis). *We visit the Body Fat Prediction Dataset (Penrose et al., 1985), which includes a response variable BodyFat and 13 covariates, such as Age, Weight, and Neck circumference, etc. We construct a binary response $Y = 1(\text{BodyFat} > 18)$ to indicate whether a man is overweight or not, and perform linear discriminant analysis (LDA). Notice that $\text{pr}(Y = 1) \approx 0.5$ for this dataset. To simplify the problem, we transform the covariate X to meet the assumption $X \sim N(0, I_p)$, allowing us to obtain the discriminant direction by*

$$\beta = E[X\{1(Y = 1) - 1(Y = 0)\}].$$

Given the sensitive information contained in each record, it is desirable to estimate β in a differentially private manner. Unfortunately, directly releasing the sample estimate of β would compromise individual privacy. To demonstrate this, we propose a tracing attack:

$$\mathcal{A}_\beta(z_0, \hat{\beta}(\mathcal{D})) = \langle x_0\{1(y_0 = 1) - 1(y_0 = 0)\} - \beta, \hat{\beta}(\mathcal{D}) \rangle,$$

where $\mathcal{D} = \{z_i : z_i \triangleq (x_i, y_i)\}_{i=1}^n$ denotes the dataset for computing $\hat{\beta}(\mathcal{D})$, $\hat{\beta}(\mathcal{D}) \triangleq \frac{1}{n} \sum_{i=1}^n x_i \{1(y_i = 1) - 1(y_i = 0)\}$, and $z_0 \triangleq (x_0, y_0)$ is a single record to be traced (i.e., to be identified $z_0 \in \mathcal{D}$ or not).

Clearly, $A_\beta(z_0, \hat{\beta}(\mathcal{D}))$ takes a large value if $z_0 \in \mathcal{D}$ and tends towards zero if $z_0 \notin \mathcal{D}$. This intuitive observation inspires us to treat $A_\beta(\cdot, \hat{\beta}(\mathcal{D}))$ as a binary classifier that outputs “in” if $A_\beta(z_0, \hat{\beta}(\mathcal{D})) > \tau$ and “out” otherwise, given a proper threshold τ . To show the effectiveness of this classifier, we conduct the following experiment. First, since β is an unknown parameter, we replace it with $x' \{1(y' = 1) - 1(y' = 0)\}$, where (x', y') is a random sample drawn from \mathcal{D} . We then randomly divide the remaining samples in \mathcal{D} into two disjoint parts of equal size, \mathcal{D}_1 and \mathcal{D}_2 . As only \mathcal{D}_1 will be utilized to calculate $\hat{\beta}$, we tag the samples in \mathcal{D}_1 with the label “in” and those in \mathcal{D}_2 with the label “out”. We can then predict the label of each datum $z_0 \in \mathcal{D}_1 \cup \mathcal{D}_2$ by computing $A_\beta(z_0, \hat{\beta}(\mathcal{D}_1))$. To evaluate the results, we plot the Receiver Operating Characteristic (ROC) curve, which allows us to avoid specifying a particular threshold τ . The red solid line in Figure 1 shows the result obtained using the raw $\hat{\beta}(\mathcal{D}_1)$, which wraps a relatively large area, indicating that A_β is an effective classifier, thus is sharp in attacking $\hat{\beta}(\mathcal{D}_1)$. In contrast, the blue dashed line, representing result obtained using a differentially private $\tilde{\beta}(\mathcal{D}_1)$ (see Section 3 for details), suggests that A_β fails to accurately identify the label of z_0 based on $\tilde{\beta}(\mathcal{D}_1)$, which means that $\tilde{\beta}(\mathcal{D}_1)$ preserves the privacy of \mathcal{D}_1 .

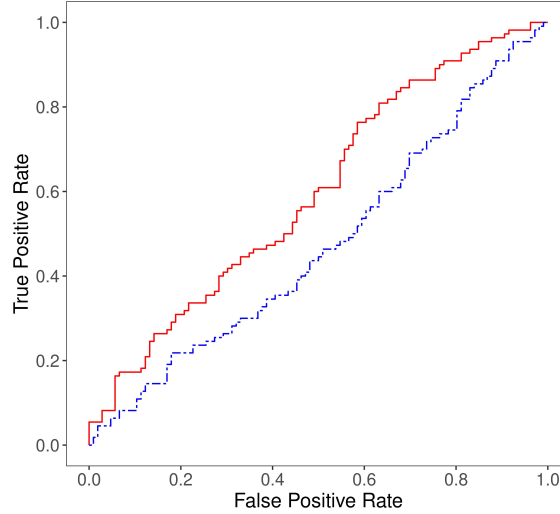


Figure 1: Tracing attack against the discriminant direction of LDA. The ROC curves depict the tracing results based on a naive estimate (red solid line) and a differentially private counterpart (blue dashed line).

The preceding example further reveals the risk of privacy leakage in releasing an unprotected estimate of the basis that spans the SDR subspace $\mathcal{S}_{Y|X}$. The risk arises because the discriminant direction obtained from linear discriminant analysis is identical to the basis provided by the celebrated sliced inverse regression (SIR, (Li, 1991)), except for scaling (Chen and Li, 2001). As SIR has played a pivotal role in sufficient dimension reduction, we are motivated to extend it for handling decentralized datasets containing sensitive information. Our approach, which we call Federated SIR (FSIR), has the following major contributions.

First, as the name implies, FSIR leverages a federated paradigm to integrate information from diverse clients to estimate the sufficient dimension reduction subspace $\mathcal{S}_{Y|X}$. In contrast to existing distributed SDR

methods that are mainly guided by the divide-and-conquer strategy to tackle massive data without considering privacy leakage during communication (Xu et al., 2022; Chen et al., 2022; Cui et al., 2023), our approach prioritizes both client-level (data ownership) and record-level (differential) privacy. While similar privacy considerations have been explored in the context of principal component analysis (PCA) (Chaudhuri et al., 2013; Jiang et al., 2016; Grammenos et al., 2020), an unsupervised counterpart of sliced inverse regression, we are not aware of any literature exploring its extension to sufficient dimension reduction. Our work shows that by combining appropriate perturbation strategies, FSIR can guarantee (ϵ, δ) -differential privacy at a low cost of statistical accuracy. In particular, we introduce a novel multivariate Gaussian mechanism specifically designed to preserve the information necessary for accurately identifying $\mathcal{S}_{Y|X}$ during the perturbation process.

Second, FSIR can handle high-dimensional data efficiently on each client. A large body of literature has contributed to estimating $\mathcal{S}_{Y|X}$ on a unified high-dimensional dataset, including early work on penalized regression-based formulations of SDR methods by Li (2007), the widely-adopted coordinate-independent sparse estimation method (CISE) by Chen et al. (2010), and the general sparse SDR framework SEAS by Zeng et al. (2022), among others. In particular, extensive studies on high-dimensional sliced inverse regression have made notable progress in both methodological development and theoretical understanding (Lin et al., 2019; Tan et al., 2018; Lin et al., 2021; Tan et al., 2020). Despite these advances, an effective strategy for producing a sparse SIR on a decentralized dataset is still lacking. Specifically, when dealing with enormous client devices, many of which have limited computation resources, it is desirable to achieve sparsity with a minimal cost on the client-side while leveraging the benefits of federated computing. To address these requirements, we propose a simple yet effective collaborative feature screening method that seamlessly integrates into the FSIR framework to yield a sparse estimator of the basis. Theoretical guarantees for this collaborative screening strategy will be discussed.

Third, FSIR is designed to be communication efficient and computational effective. Compared with multi-round optimization-based approaches (Cui et al., 2023), FSIR achieves communication efficiency through a one-shot aggregation of local estimates from collaborative clients, thus circumvents introducing noises in each optimization step (Abadi et al., 2016). Moreover, the primary computation cost on each client is attributed to performing singular value decomposition on two low-dimensional matrices, leading to computational effectiveness. These characteristics make FSIR well-suited for applications on edge devices, such as smartphones, where efficient and privacy-preserving computations are crucial.

The following notation will be used in this paper. For a positive integer H , we write $[H]$ as shorthand for $\{1, \dots, H\}$. For a vector $\beta \in \mathbb{R}^p$ and a subset $\mathcal{I} \subseteq [p]$, we use $\beta_{\mathcal{I}}$ to denote the restriction of vector β to the index set \mathcal{I} . In addition, we write $\text{supp}(\beta) := \{j \in [p] : \beta_j \neq 0\}$. For two vectors β_1 and β_2 of same dimension, denote the angle between them by $\angle(\beta_1, \beta_2)$. For $x \in \mathbb{R}^p$ and $R > 0$, let $\Pi_R(x)$ denote the projection of x onto the l_2 ball $\{u \in \mathbb{R}^p : \|u\|_2 \leq R\}$. Define a multiset as an ordered pair (\mathcal{B}, m) where \mathcal{B} is the underlying set formed of distinct elements and $m : \mathcal{B} \rightarrow \mathbb{Z}^+$ is the function giving the multiplicity of an element in \mathcal{B} . For two sets \mathcal{B}_1 and \mathcal{B}_2 , denote their multiset sum by $\mathcal{B}_1 \uplus \mathcal{B}_2$. For a parameter $\theta \in \Theta$, $\hat{\theta}$ denotes a raw estimator and $\tilde{\theta}$ denotes a differentially private estimator.

2 Problem Formulation

2.1 Preliminaries

We revisit the concept of differential privacy before moving on. Intuitively, the privacy level set (δ, ϵ) in definition (1) measures how much information $\mathcal{M}(\cdot)$ reveal about any individual record in the dataset \mathcal{D} , where the smaller value of ϵ or δ imposes the more stringent privacy constraint. This definition leads to

some nice properties of differential privacy. The two most useful ones are listed as follows, which provide a convenient way to construct complex differentially private algorithms.

Property 1 (Post-processing property, Dwork et al. (2006)). *If $\mathcal{M} : \mathcal{X}^n \rightarrow \Theta_0$ is (ϵ, δ) -differentially private and $\mathcal{M}' : \Theta_0 \rightarrow \Theta_1$ is any randomized algorithm, then $\mathcal{M}' \circ \mathcal{M}$ is (ϵ, δ) -differentially private.*

Property 2 (Composition property, Dwork et al. (2006)). *Let \mathcal{M}_i be (ϵ_i, δ_i) -differentially private for $i = 1, 2$, then $\mathcal{M}_1 \circ \mathcal{M}_2$ is $(\epsilon_1 + \epsilon_2, \delta_1 + \delta_2)$ -differentially private.*

A standard approach for developing differentially private algorithms involves introducing random noises to the output of their non-private counterparts, see (Dwork et al., 2014). One such technique, known as the Gaussian mechanism, employs independently and identically distributed (i.i.d.) Gaussian noise. The noise's scale is governed by the l_2 sensitivity of the algorithm, which quantifies the maximum change in the algorithm's output resulting from substituting a single record in its input data set. The formal definition is presented below.

Definition 1 (l_2 -sensitivity). *For an algorithm $f : \mathcal{D} \rightarrow \mathbb{R}^p$, its l_2 -sensitivity is defined as*

$$\Delta_2(f) = \sup_{\mathcal{D}, \mathcal{D}'} \|f(\mathcal{D}) - f(\mathcal{D}')\|_2,$$

where $\mathcal{D}, \mathcal{D}' \in \mathcal{X}^n$ are datasets differing in a single record.

Definition 2 (Gaussian mechanism). *For any vector-valued algorithm $f : \mathcal{D} \rightarrow \mathbb{R}^p$ which satisfies $\Delta_2(f) < \infty$, the Gaussian mechanism is defined as*

$$\tilde{f}(\mathcal{D}) \triangleq f(\mathcal{D}) + \xi,$$

where $\xi \triangleq (\xi_1, \xi_2, \dots, \xi_p)$ and $\xi_j, j \in [p]$ is an i.i.d. sample drawn from $\mathcal{N}(0, \sigma_\xi^2)$.

Next we briefly review sliced inverse regression. Let $Y \in \mathbb{R}$ be a response variable and $X = (X_1, \dots, X_p)^\top \in \mathbb{R}^p$ be the associated covariates, with covariance matrix $\Sigma = \text{cov}(X)$. Assume the SDR subspace $\mathcal{S}_{Y|X} = \text{span}(\beta)$, where $\beta \in \mathbb{R}^{p \times d}$ is the basis matrix and d ($d < p$) is the structure dimension. SIR seeks for an unbiased estimate of $\mathcal{S}_{Y|X}$. Without loss of generality, assume Y is categorical with H fixed classes, denoted as $Y \in [H]$; otherwise, we simply follow Li (1991) to construct a discrete version \tilde{Y} of Y by partitioning its range into H slices without overlapping. This discretization operation will not lose information for estimating SDR subspace, i.e., $\mathcal{S}_{\tilde{Y}|X} = \mathcal{S}_{Y|X}$, given H sufficiently large (Bura and Cook, 2001). In preparation, let $p_h \triangleq \text{pr}(Y = h)$ and $m_h^0 \triangleq E\{X - E(X)|Y = h\}$, the kernel matrix is then given by

$$\Lambda^0 \triangleq \sum_{h=1}^H p_h m_h^0 m_h^{0\top}.$$

Li (1991) has shown that, if X satisfies the so-called linear conditional mean (LCM) condition, i.e., $E(X | \beta^\top X)$ is a linear function of $\beta^\top X$, then $\Sigma^{-1} m_h^0 \in \mathcal{S}_{Y|X}$, $h \in [H]$. This result implies that $\Sigma^{-1} \text{col}(\Lambda^0) \subseteq \mathcal{S}_{Y|X}$. In practice, we further assume the coverage condition, that is, $\Sigma^{-1} \text{col}(\Lambda^0) = \mathcal{S}_{Y|X}$, so the first d eigenvectors of $\Sigma^{-1} \text{col}(\Lambda^0)$ spans $\mathcal{S}_{Y|X}$ and the remaining $p - d$ eigenvalues equal to zero.

At the sample level, we can compute the plug-in estimator $\hat{\Sigma}$ and $\text{col}(\hat{V}_H^0)$ to estimate $\mathcal{S}_{Y|X}$, where \hat{V}_H^0 is the matrix formed by the top d principal eigenvectors of $\hat{\Lambda}^0$. Lin et al. (2018) has shown that the space spanned by $\hat{\Sigma}^{-1} \hat{V}_H^0$ yields a consistent estimate of $\mathcal{S}_{Y|X}$ if and only if $\rho_n := \frac{p}{n} \rightarrow 0$ as $n \rightarrow \infty$, when the slice number H is a fixed integer independent of n and p , and the structure dimension d is bounded.

2.2 Computing SIR in a federated paradigm

Consider a dataset $\mathcal{D} \triangleq \{\mathcal{D}^{(1)} \mid \dots \mid \mathcal{D}^{(K)}\}$ distributed across K clients, where $\mathcal{D}^{(k)} = \{(x_i, y_i) : x_i \in \mathbb{R}^p, y_i \in [H]\}_{i=1}^{n_k}$ is the subset stored on the k th client of with n_k samples, $k \in [K]$. Let $N = \sum_{k=1}^K n_k$ be the total size of \mathcal{D} . Generally, we do not require $n_k > p$ for any single client $k \in [K]$, thus on some or even all clients, data may follow a high-dimensional setting ($p > n_k$, or $p \gg n_k$). Meanwhile, given K sufficiently large, it is also reasonable to assume a low-dimensional setting for the whole dataset \mathcal{D} , that is, $p < N$.

To handle this decentralized dataset, we need modify the classical SIR method slightly. Denote $m_h \triangleq E[\{X - E(X)\}1(Y = h)]$, we immediately have $\Sigma^{-1}m_h \in \mathcal{S}_{Y|X}$ for $h \in [H]$, since $m_h = p_h m_h^0$. For convenience of expression, define the slice mean matrix $M \triangleq (m_1, \dots, m_H) \in \mathbb{R}^{p \times H}$ and the kernel matrix $\Lambda \triangleq MM^\top$, then

$$\Sigma^{-1} \text{col}(\Lambda) = \mathcal{S}_{Y|X}. \quad (3)$$

Using Λ instead of Λ^0 offers several benefits in our federated computation. The first advantage arises in scenarios with imbalanced classes, where a client only has a small portion of observations for certain classes. Estimating Λ^0 in such cases can be highly unstable, resulting in a biased global estimator. This situation is frequently encountered in streaming data, as discussed by Cai et al. (2020) in developing their online SIR estimator. In our problem, utilizing Λ further allows us to eliminate privacy leakage in uploading \hat{p}_h 's, thus avoiding unnecessary complexities in both algorithm design and theoretical analysis. Additionally, as detailed in Section 3, Λ has a smaller l_2 -sensitivity, reducing the noise scale required for perturbation strategies.

Algorithm 1 presents a federated framework for computing SIR on a decentralized dataset \mathcal{D} , catching a glimpse of our FSIR method. In this framework, each client $k \in [K]$ operates independently to estimate the slice mean matrix as $\widehat{M}^{(k)}$ and the covariance matrix as $\widehat{\Sigma}^{(k)}$ based on their local dataset $\mathcal{D}^{(k)}$, without needing to access external data. Subsequently, these two matrices are uploaded to the central server after a perturbation operation to ensure differential privacy (see details later). A global estimate of the SDR subspace is obtained on the server in Step 4, achieved through the merging of $\widehat{M}^{(k)}$ and $\widehat{\Sigma}^{(k)}$ for all $k \in [K]$, where $\widehat{M}^{(k)}$ and $\widehat{\Sigma}^{(k)}$ denoting the perturbed matrices.

At first glance, the pooling and averaging operations at Step 2 and 3 on the server might suggest that FSIR is merely another application of the FedAvg algorithm (McMahan et al., 2017). However, FSIR distinguishes itself by emphasizing on one-shot communication and, more importantly, privacy protection. Throughout the procedure, each client only computes and uploads local model estimates to the server, ensuring that sensitive records would remain localized with their owner. In this way, FSIR restricts the central server or any other client j can only probe the dataset of client k through its uploaded estimates. Meanwhile, admitting the existence of potential malicious participants who may conduct tracing attacks on the shared estimates, FSIR necessitates the differential privacy of both $\widehat{M}^{(k)}$ and $\widehat{\Sigma}^{(k)}$. This privacy requirement ensures that any operation performed on these estimates does not cause additional privacy breaches, thanks to the post-processing property of differential privacy.

An essential step in Algorithm 1 involves the construction of differentially private $\widetilde{\Sigma}^{(k)}$ and $\widetilde{M}^{(k)}$ for each client k . Privacy-preserving estimation of covariance matrices has been extensively studied, as evidenced by a large body of literature (Chaudhuri et al., 2012; Grammenos et al., 2020; Biswas et al., 2020; Wang and Xu, 2021). While it is not the primary focus of this paper, we adapt the approach suggested by Grammenos et al. (2020) within our framework, corresponding to Step 3 on the client and Step 2 on the server. The following lemma guarantees the differential privacy of $\widetilde{\Sigma}^{(k)}$. In the next section, our attention will shift towards the development of a differentially private slice mean matrix, whose singular subspace plays a crucial role in

Algorithm 1: The FSIR framework.

Data: $\mathcal{D} = \bigcup_{k=1}^K \mathcal{D}^{(k)}$
Input: Clients number K , privacy level sets (ϵ_x, δ_x) and (ϵ_m, δ_m) .
Client $k \in [K]$ **do in parallel**
 1. **if** $p > n_k$ **then**
 */*An alternative step to tackle high-dimensional data.*/*
 Estimate local active variable set $\mathcal{A}^k \leftarrow$ CCMD-Filter (Section 3.3);
 Upload $\mathcal{A}^{(k)}$ and pull \mathcal{A} from Server;
 $X^{(k)} \leftarrow X_{\mathcal{A}}^{(k)}$;
 end
 2. Upload the private slice mean matrix $\widetilde{M}^{(k)}$ (Section 3.1 or 3.2);
 3. Compute the private covariance matrix $\widetilde{\Sigma}^{(k)}$ to perform $(\widetilde{U}_x^{(k)}, \widetilde{S}_x^{(k)}, \widetilde{V}_x^{(k)}) \leftarrow \text{SVD}(\widetilde{\Sigma}^{(k)})$,
 then upload $(\widetilde{U}_x^{(k)}, \widetilde{S}_x^{(k)})$;
end
Server do
 1. **if** $\mathcal{A}^{(k)} \neq \emptyset$ **then**
 */*An alternative step to tackle high-dimensional data.*/*
 Update $\mathcal{A} \leftarrow$ CCMD-Filter (Algorithm 3);
 end
 2. Merge $\widetilde{X} = [\widetilde{U}_x^{(1)} \widetilde{S}_x^{(1)} \mid \widetilde{U}_x^{(2)} \widetilde{S}_x^{(2)} \mid \dots \mid \widetilde{U}_x^{(K)} \widetilde{S}_x^{(K)}]$ to obtain $\widetilde{\Sigma} = \frac{1}{N} \widetilde{X} \widetilde{X}^\top$;
 3. Merge $\widetilde{M} = \frac{1}{K} \sum_{k=1}^K \widetilde{M}^{(k)}$ to obtain $(\widetilde{U}_M, \widetilde{S}_M, \widetilde{V}_M) \leftarrow \text{SVD}(\widetilde{M})$;
 4. Return the global estimate $\widetilde{\beta} = \widetilde{\Sigma}^{-1} \widetilde{U}_M$.
end

estimating $\mathcal{S}_{Y|X}$.

Lemma 1. (Chaudhuri et al., 2012) Let $X \in \mathbb{R}^{p \times n}$ be the centralized design matrix on the client with $\|X_i\| \leq 1$ for all $i \in [n]$. Denote $\widehat{\Sigma} = \frac{1}{n} X X^\top$. Let $A \in \mathbb{R}^{p \times p}$ be a symmetric random matrix whose entries are i.i.d. drawn from $N(0, \sigma_x^2)$, where

$$\sigma_x = \frac{p+1}{n\epsilon_x} \left\{ 2 \log \left(\frac{p^2+p}{\delta 2\sqrt{2\pi}} \right) \right\} + \frac{1}{n\epsilon_x^{1/2}}.$$

Then $\widetilde{\Sigma} \triangleq \widehat{\Sigma} + A$ is (ϵ_x, δ_x) -differentially private.

3 Estimation with differential privacy

3.1 Private slice mean matrix: a preliminary way

On the client-side, a natural approach for constructing a differential private slice mean matrix is to apply the i.i.d. Gaussian mechanism to the mean vector of each slice; see Proposition 2, which can be easily derived from Theorem A.1 in Dwork et al. (2014).

Proposition 2. Let $\{(X_i, y_i)^T \in \mathbb{R}^{n \times (p+1)}, i \in [n]\}$ be i.i.d. samples on a client. Denote $\hat{m}_h \triangleq \frac{1}{n} \sum_{i=1}^n X_i 1(y_i = h)$ and assume its l_2 -sensitivity $\Delta_2 < \infty$. Define $\tilde{m}_h \triangleq \hat{m}_h + (\xi_1, \xi_2, \dots, \xi_p)^T \in \mathbb{R}^p$, where $\xi_j \sim N(0, \frac{\Delta_2^2 \log(1/\delta)}{\epsilon^2})$, then $\tilde{M} \triangleq (\tilde{m}_1, \dots, \tilde{m}_H) \in \mathbb{R}^{p \times H}$ is (ϵ, δ) -differentially private.

Clearly, the noise scale is determined by both of the privacy level set (ϵ, δ) and the l_2 -sensitivity Δ_2 . Recall that sliced inverse regression usually assumes that X is integrable and has an elliptical distribution to satisfy the LCM condition, which does not guarantee $\Delta_2 < \infty$ in general. Therefore, we truncate X to restrict it on a finite support. Given the truncation level R , let

$$\bar{m}_{h,j} = \frac{1}{n} \sum_{i=1}^n \Pi_R(X_{ij} 1(y_i = h)), j \in [p].$$

Denote $\bar{m}_h = (\bar{m}_{h,1}, \dots, \bar{m}_{h,p})^T$ and $\bar{M} \triangleq (\bar{m}_1, \dots, \bar{m}_H) \in \mathbb{R}^{p \times H}$. We then utilize \bar{M} rather than \hat{M} to meet the assumption $\Delta_2 < \infty$. More precisely, since a sample can be only located in one slice, we easily obtain $\Delta_2 = 2R\sqrt{p}/n_0$ over a pair of data sets which only differ by one single entry, where n_0 is the minimal sample size of slices.

Notice the differential privacy is always guaranteed at the expense of estimation accuracy (Wasserman and Zhou, 2010; Bassily et al., 2014). In real applications, a client could have extremely limited observations, causing the scale of added noises significantly larger than of the signal. For this, we suggest to set an upper bound σ_0^2 as a tolerated scale of noise and calculate the minimal sample size

$$n_{\epsilon, \delta, p, R} = \frac{R\sqrt{p \log(1/\delta)}}{\sigma_0 \epsilon}$$

required by each client. Thus for client $k \in [K]$, only if $n_k \geq n_{\epsilon, \delta, p, R}$, we compute and upload \tilde{M}_k following Proposition 2.

Remark. The truncating operation is widely adopted for both theoretical studies and practical applications, we refer to (Lei, 2011; Cai et al., 2021) for more details on choosing a proper truncation level. As for the selection of privacy level set, we adopt convention $\epsilon \in \{0.5, 1\}$ and $\delta = 1/n^{1.1}$ for simplicity, which are usually considered as the largest value to provide a nontrivial privacy protection (Dwork et al., 2014).

3.2 Private slice mean matrix: singular space oriented

The use of vanilla Gaussian mechanism in the previous section is intuitive and simple, yet has a significant limitation: it does not account for the impact of perturbation operation on the left singular space of \bar{M} , which is crucial for estimating $\mathcal{S}_{Y|X}$, as revealed by (3). To mitigate this, we propose a novel perturbation strategy, termed multivariate Gaussian (MVG) mechanism, to provide (ϵ, δ) -differential privacy for \bar{M} without sacrificing too much information we needed. We start by giving its definition.

Definition 3 (Multivariate Gaussian mechanism). For any vector-valued algorithm $f : \mathcal{D} \rightarrow \mathbb{R}^p$ which satisfies $\Delta_2(f) < \infty$, define the multivariate Gaussian mechanism as

$$\tilde{f}(\mathcal{D}) \triangleq f(\mathcal{D}) + \xi,$$

where $\xi \sim \mathcal{N}_p(0, \Sigma_\xi)$.

Obviously, the noise vector ξ is characterized by the covariance matrix Σ_ξ . In particular, if $\Sigma_\xi = \frac{\Delta_2^2 \log(1/\delta)}{\epsilon^2} I_p$, the MVG mechanism coincides with the i.i.d. Gaussian mechanism. The theorem below provides a sufficient condition for holding the (ϵ, δ) -differential privacy of MVG mechanism.

Theorem 3. Let $\{(X_i, y_i)^\top \in \mathbb{R}^{n \times (p+1)}, i \in [n]\}$ be i.i.d. samples on a client. Denote $\hat{m}_h \triangleq \frac{1}{n} \sum_{i=1}^n X_i 1(y_i = h)$ and assume its l_2 -sensitivity $\Delta_2 < \infty$. Define $\tilde{m}_h \triangleq \hat{m}_h + \xi \in \mathbb{R}^p$, where $\xi \sim \mathcal{N}_p(0, \Sigma_\xi)$. Suppose the eigen value decomposition $\Sigma_\xi = U_\xi D_\xi U_\xi^\top$. Then $\tilde{M} \triangleq (\tilde{m}_1, \dots, \tilde{m}_H) \in \mathbb{R}^{p \times H}$ is (ϵ, δ) -differentially private, if D_ξ satisfies

$$\left\| D_\xi^{-1} \right\|_F \leq \frac{4 \log \frac{2}{\delta} + 2\epsilon - 4\{(\log \frac{2}{\delta})^2 + \log \frac{2}{\delta} \epsilon\}^{1/2}}{\Delta_2^2}.$$

By Taylor expansion and some algebraic computations, we can further obtain

$$\frac{4 \log \frac{2}{\delta} + 2\epsilon - 4\{(\log \frac{2}{\delta})^2 + \log \frac{2}{\delta} \epsilon\}^{1/2}}{\Delta_2^2} \approx \frac{\epsilon^2}{2\Delta_2^2 \log \frac{2}{\delta}} \approx \frac{n_{\epsilon, \delta, p, R}^2 \epsilon^2}{8R^2 p \log \frac{2}{\delta}},$$

where $n_{\epsilon, \delta, p, R}$ is the minimum sample size on the client. For expression convenience, we use

$$\Upsilon_{mvg} \triangleq \frac{n_{\epsilon, \delta, p, R}^2 \epsilon^2}{8R^2 p \log \frac{2}{\delta}} \quad (4)$$

as an approximate upper bound of $\left\| D_\xi^{-1} \right\|_F$.

Theorem 3 presents an inspiring result that allows for flexible design of the eigenvectors U_ξ while achieving differential privacy by bounding $\left\| D_\xi^{-1} \right\|_F$. Building upon this finding, we proceed by performing singular value decomposition on \bar{M} , yielding $\bar{M} = W_1 S W_2^\top$. We take $U_\xi = W_1$ and sorting the diagonal elements of D_ξ in the same order as the diagonal elements of S , while enforcing the constraint $\left\| D_\xi^{-1} \right\|_F \leq \Upsilon_{mvg}$. The key idea here is to construct a p -dimensional noise vector ξ with a specific covariance structure, such that its eigenspace aligns with the left singular subspace of the slice mean matrix \bar{M} . Thus the perturbed matrix $\tilde{M} = \bar{M} + E_0$ can preserve the relevant information about $S_{Y|X}$, where E_0 is a noise matrix whose columns are generated from ξ .

Algorithm 2 outlines more details about our strategy. Steps 1 to 3 involve splitting the left singular space of \bar{M} into two parts: a d -dimensional subspace spanned by the leading singular vectors and its orthogonal complement. Since the first part will be utilized to construct $S_{Y|X}$, we preserve these eigenvectors and maintain their ordering based on corresponding eigenvalues. Meanwhile, to ensure that $\Sigma_\xi \succ 0$, we suggest that the eigenvectors in the second part have no significant difference and share the same eigenvalue. Following this, Steps 4 to 6 construct a diagonal matrix S' by appropriately allocating Υ_{mvg} , which guarantees that $\Sigma_\xi = W_1 S'^2 W_1^\top$ and $\left\| \Sigma_\xi^{-1} \right\|_F = \Upsilon_{mvg}$. Finally, Steps 7 and 8 involve generating multivariate Gaussian samples and uploading perturbed slice mean matrix.

Remark. Step 3 in Algorithm 2 aims to estimate the structure dimension d by simply ranking the eigen-gaps of \bar{M} . This approach avoids any additional computational burden. However, alternative methods are available for determining the structure dimension, and we refer interested reader to (Luo and Li, 2021) for a detailed study.

Algorithm 2: Compute private slice mean matrix via the MVG mechanism.

Data: $\mathcal{D} = \{(X_i, y_i) \in \mathbb{R}^{p+1}, i \in [n]\}$.

Input: Privacy level set (ϵ, δ) , truncation level R .

Output: Perturbed slice mean matrix $\widetilde{M} \in \mathbb{R}^{p \times H}$.

1. Compute the truncated slice mean matrix \overline{M} ;
2. Obtain $(W_1, S, W_2^T) \leftarrow \text{SVD}(\overline{M})$, where $S \in \mathbb{R}^{p \times p}$. Denote the j th diagonal element of S by s_j , $j \in [p]$;
3. Estimate the structure dimension d by ranking eigengaps of s_j , $j \in [p]$;
4. Compute the approximated upper bound Υ_{mvg} ;
5. Compute $s_{\perp} \triangleq \sum_{j=\widehat{d}+1}^p s_j / (p - \widehat{d})$ and construct a sequence of pseudo eigenvalues

$$s' \triangleq (s_1, \dots, s_{\widehat{d}}, \underbrace{s_{\perp}, \dots, s_{\perp}}_{p-\widehat{d}})^T \in \mathbb{R}^p$$

to obtain the ratio vector $r = (r_1, \dots, r_p)^T$, where $r_j = \frac{1/s'_j}{\sum_{j=1}^p s'_j}$;

6. Construct a diagonal matrix $S' \in \mathbb{R}^{p \times p}$ with the j th diagonal element

$$s'_j = \frac{1}{\sqrt{\Upsilon_{mvg} r_j}}, j \in [p];$$

7. Generate a matrix $Z \in \mathbb{R}^{p \times H}$, where $Z_{j,h} \sim_{i.i.d.} N(0, 1)$ for $j \in [p]$, $h \in [H]$;
8. Obtain

$$E_0 \triangleq W_1 S' Z \in \mathbb{R}^{p \times H}$$

and upload $\widetilde{M} \triangleq \widehat{M} + E_0$.

Remark. Compared with the i.i.d. Gaussian mechanism, the MVG mechanism preserves the information carried by the left singular subspace of \overline{M} at the cost of a higher variance of noise. To see this, we calculate $\sigma_{mvg}^2 = \frac{2p\Delta_2^2 \log(2/\delta)}{\epsilon^2}$, which mimics an i.i.d. noise setting under the constraint (4). Clearly, this variance is significantly larger than $\frac{\Delta_2^2 \log(1/\delta)}{\epsilon^2}$ stated in Proposition 2, particularly when p is large. Section 5 will compare two mechanisms in details.

Remark. Note that we further have

$$\|\Sigma_{\xi}\|_2 \geq \frac{8R^2 p \log \frac{2}{\delta}}{n_{\epsilon, \delta, p, R}^2 \epsilon^2}$$

and the minimum is reached if all the eigenvalues of Σ_{ξ} are the same. In practice, we choose the scale of $\|\Sigma_{\xi}\|_2$ exactly as $CR^2 p \log \frac{2}{\delta} / (n_{\epsilon, \delta, p, R}^2 \epsilon^2)$, where constant $C \geq 8$. In order to keep the noise from drowning out the signal, we need to make sure that the client sample size is large enough, that is

$$\frac{CR^2 p \log \frac{2}{\delta}}{n_{\epsilon, \delta, p, R}^2 \epsilon^2} = o(1).$$

This condition is required for our theoretical study.

3.3 Sparse estimation in the high-dimensional setting

In many scenarios, client data can be high-dimensional ($p > n$) or even ultra-high-dimensional ($p = o(\exp(n^\alpha))$). Since SIR relies on $p/n \rightarrow 0$ as $n \rightarrow \infty$ to guarantee the consistency of \hat{V}_H (Lin et al., 2018), we require a feature screening step as an initial operation to handle these data. Recall that SIR is developed upon the observation that $\Sigma^{-1}\{E(X|Y) - E(X)\} \in \mathcal{S}_{Y|X}$, implying that $\mathcal{S}_{Y|X}$ degenerates if $E(X|Y) - E(X) = 0$ almost surely. This allows us to define the active set as

$$\mathcal{T} = \{j \in [p] \mid E(X_j|Y) \neq E(X_j) \text{ a.s.}\}$$

and utilize the following criterion for screening

$$\omega_{j,h} \triangleq |E\{X_j - E(X_j)|Y = h\}|, \quad h \in [H].$$

To fully utilize the information from decentralized data, we compute $\omega_{j,h}^{(k)}$ on each client $k \in [K]$ and perform the screening process on the server. This screening technique, known as the Collaborative Conditional Mean Difference (CCMD) filter, is designed to operate under a federated paradigm. We clarify its implementation details in Algorithm 3. With the inclusion of the CCMD filter, our FSIR framework now successfully handles high-dimensional data and is fully operational.

Algorithm 3: The collaborative conditional mean difference (CCMD) filter.

Data: $\mathcal{D} = \bigcup_{k=1}^K \mathcal{D}^{(k)}$.

Input: threshold c , slice number H , client number K .

Output: Estimated active set $\hat{\mathcal{T}}$.

Client $k \in [K]$ do in parallel:

1. Compute $\Omega^{(k)} \in \mathbb{R}^{p \times H}$ where $\Omega_{j,h}^{(k)} \triangleq |\hat{m}_{h,j}^{(k)}|$;
2. **For label $h \in [H]$:**
 - Estimate the active set on h th slice $\hat{\mathcal{T}}_h^{(k)} \triangleq \{j \in [p] \mid \Omega_{j,h}^{(k)} > c\}$;
- end**
3. Upload the k th multiset $\mathcal{B}^{(k)} \triangleq \biguplus_{h \in [H]} \hat{\mathcal{T}}_h^{(k)}$;

end

Server do:

4. Obtain the global multiset $\mathcal{B} \triangleq \biguplus_{k \in [K]} \mathcal{B}^{(k)}$;
5. Return the global active set $\hat{\mathcal{T}} \triangleq \{j \in \mathcal{B} \mid \text{multiplicity}(j) > \frac{K}{2}\}$.

end

Remark. Step 3 of Algorithm 3 does not involve privacy leakage, since this operation only uploads an index set of possible active variables rather than their mean values. For the later case, Dwork et al. (2018) has developed a differentially private approach, named “Peeling”, to estimate the top- s largest elements in a p -dimensional mean vector.

4 Theoretical analysis

We focus on the homogeneous scenario where all client share the same SDR subspace, and defer the homogeneous case to future research because of the additional technical challenges associated with it. Without

loss of generality, we suppose $E(x) = 0$, and the sample sizes of all the slices are same, that is $n_{k0} = n_k/H$. Lin et al. (2018) imposed the following conditions required in high-dimensional slice inverse regression.

Condition 1. For any $\zeta \in \mathbb{R}^p$, $E(\zeta^\top x | \beta_1^\top x, \dots, \beta_d^\top x)$ is a linear combination of $\beta_1^\top x, \dots, \beta_d^\top x$.

Condition 2. The dimension of the space spanned by the central curve equals the dimension of the central space, i.e., $d' = d$.

Condition 3. x is sub-Gaussian and there exist positive constants C_1, C_2 such that

$$C_1 \leq \lambda_{\min}(\Sigma) \leq \lambda_{\max}(\Sigma) \leq C_2,$$

where $\lambda_{\min}(\Sigma)$ and $\lambda_{\max}(\Sigma)$ are the minimal and maximal eigenvalues of Σ respectively.

Condition 4. The central curve $m(y) \triangleq E(x|y)$ has finite fourth moment and is ν -sliced stable (defined below) with respect to y and $m(y)$.

Definition 4. For two positive constants $\gamma_1 < 1 < \gamma_2$, let $\mathcal{A}_H(\gamma_1, \gamma_2)$ be the collection of all the partition $-\infty = a_0 < a_1 < \dots < a_H = \infty$ of \mathbb{R} satisfying that

$$\frac{\gamma_1}{H} \leq \text{pr}(a_i \leq y < a_{i+1}) \leq \frac{\gamma_2}{H}.$$

The central curve $m(y) = E(x|y)$ is called ν -sliced stable with respect to y for some $\mu > 0$ if there exist positive constants $\gamma_i, i = 1, 2, 3$ such that for any β in the central space for any partition in $\mathcal{A}_H(\gamma_1, \gamma_2)$, we have

$$\frac{1}{H} \left| \sum_{h=0}^{H-1} \text{var}\{\beta^\top m(y) | a_h \leq y \leq a_{h+1}\} \right| \leq \frac{\gamma_3}{H^\nu} \text{var}\{\beta^\top m(y)\}.$$

The central curve is sliced stable if it is ν -sliced stable for some positive constant ν .

Condition 5. $s = |\mathcal{S}| \ll p$ where $\mathcal{S} = \{i | \beta_j(i) \neq 0 \text{ for some } j, 1 \leq j \leq d\}$ and $|\mathcal{S}|$ is the number of elements in the set of $|\mathcal{S}|$.

$$\mathcal{U}(\varepsilon_0, \alpha, C) = \left\{ \Sigma : \max_j \sum_i \{|\sigma_{i,j}| : |i - j| > l\} \leq Cl^{-\alpha} \text{ for all } l > 0, \right. \\ \left. \text{and } 0 < \varepsilon_0 \leq \lambda_{\min}(\Sigma) \leq \lambda_{\max}(\Sigma) \leq \frac{1}{\varepsilon_0} \right\},$$

Condition 6. $\Sigma \in \mathcal{U}(\varepsilon_0, \alpha, C)$ and $\max_{1 \leq i \leq p} r_i$ is bounded where r_i is the number of non-zero elements in the i th row of Σ .

Assumption 1. Signal strength: $\exists C > 0$ and $\omega > 0$ such that $\text{var}[E\{x(k)|y\}] > Cs^{-\omega}$ when $E\{x(k)|y\}$ is not a constant.

By the algorithm in Section 3, we can write

$$\widetilde{M} = \frac{\sum_{k=1}^K n_k \widetilde{M}^{(k)}}{\sum_{k=1}^K n_k} = \frac{\sum_{k=1}^K n_k \widehat{M}^{(k)}}{\sum_{k=1}^K n_k} + \frac{\sum_{k=1}^K n_k E_0^{(k)}}{\sum_{k=1}^K n_k},$$

and $\widehat{\Lambda} = \widetilde{M} \widetilde{M}^\top$. Now we are ready to state the main theoretical results of FSIR.

Theorem 4. Under conditions 1-4, if $n_{\epsilon, \delta, p, R}^2 \epsilon^2 (R^4 H^{2\nu-1} p^3 \log \frac{2}{\delta})^{-1} \rightarrow \infty$, then we have

$$\|\hat{\Lambda} - \Lambda_p\|_2 = O_p \left(\frac{1}{H^\nu} + \frac{H^2 p}{n} + \frac{H p^{1/2}}{n^{1/2}} \right). \quad (5)$$

Remark. We insert the discussion of convergence rate here (Remark 3 of Lin et al. (2018)).

From Section 2.2 we know that

$$\hat{\Sigma} = \frac{1}{n} X X^T + A,$$

where A is a symmetric random Gaussian matrix and $A_{i,j} \sim \mathcal{N}(0, \sigma_x^2)$ for $i \geq j$ where

$$\sigma_x = \frac{p+1}{n\epsilon_x} \left\{ 2 \log \left(\frac{p^2+p}{2\delta\sqrt{2\pi}} \right) \right\}^{1/2} + \frac{1}{n\epsilon_x^{1/2}}$$

Then we have the following Lemma:

Lemma 5. Under condition 3, we have

$$\|\hat{\Sigma} - \Sigma\|_2 \rightarrow 0$$

when $p/n \rightarrow 0$ and $n \rightarrow \infty$. It is also easy to see that

$$\|\hat{\Sigma}^{-1} - \Sigma^{-1}\|_2 \rightarrow 0.$$

Theorem 6. Under conditions 1-4 and assuming that $p/n \rightarrow 0$, we have

$$\|\hat{\Sigma}^{-1} \hat{\Lambda} - \Sigma^{-1} \Lambda_p\|_2 \rightarrow 0$$

as $n \rightarrow \infty$ with probability converging to one.

Let the sample mean in the h th slice be \bar{x}_h , and we define the inclusion set and exclusion set below, which depend on a thresholding value t ,

$$\mathcal{T} = \{j | E\{x(j)|y\} \text{ is not a constant} \},$$

$$\mathcal{I}_h = \{j | |\bar{x}_h(j)| > t\}, h = 1, \dots, H.$$

$$\mathcal{I} = \cup_h \mathcal{I}_h = \{j | \text{there exists a } h \in [1, H], \text{ s.t. } |\bar{x}_h(j)| > t\},$$

$$\mathcal{I}^c = \{j | \text{for all } h \in [1, H], |\bar{x}_h(j)| < t\}.$$

Furthermore, we write the smallest sample size of slices as $n_{\epsilon, \delta, s, R}$ in high dimension settings.

Proposition 7. *Under condition 1 - 6 and assumption 1, and let $t = Cs^{-\omega/2}$ for some constant $C > 0$ such that $t < 2C_\mu s^{-\omega/2}$, we have*

i) $\mathcal{T} \subset \mathcal{I}$ holds with probability at least

$$1 - C_1 \exp \left\{ -C_2 \frac{n_{\epsilon, \delta, s, R} s^{-\omega}}{H \nu^2} + C_3 \log(H) + C_4 \log(s) \right\} \\ - C_5 \exp \left\{ \frac{-n_{\epsilon, \delta, s, R} s^{-\omega}}{2CH\tau^2 + 2s^{-\frac{\omega}{2}}\tau} + C_6 \log(s) + C_7 \log(H) \right\}.$$

ii) $\mathcal{T}^c \subset \mathcal{I}^c$ holds with probability at least

$$1 - C_1 \exp \left\{ \frac{-n_{\epsilon, \delta, s, R} s^{-\omega}}{2CH\tau^2 + 2s^{-\frac{\omega}{2}}\tau} + C_2 \log(H) + C_3 \log(p - cs) \right\}.$$

This Proposition has a simple implication. We may choose

$$H = o(Cn_{\epsilon, \delta, s, R} s^{-\omega} \tau^{-2} / \log p)$$

so that

$$\frac{Cn_{\epsilon, \delta, s, R} s^{-\omega}}{H\tau^2} \gg \log p.$$

Theorem 8. *Let $\mathcal{T}_0 = \{j \mid \text{multiplicity}(j) > \frac{K}{2}\}$, we have*

i) $\mathcal{T} \subset \mathcal{T}_0$ holds with probability at least

$$1 - CsK^{3/2} \left(\frac{K^2 p_1}{e^2} \right)^{K/2},$$

where

$$p_1 = C_1 \exp \left\{ -C_2 \frac{n_{\epsilon, \delta, s, R} s^{-\omega}}{H \nu^2} + C_3 \log(H) \right\} + C_4 \exp \left\{ \frac{-n_{\epsilon, \delta, s, R} s^{-\omega}}{2CH\tau^2 + 2s^{-\frac{\omega}{2}}\tau} + C_5 \log(H) \right\}.$$

ii) $\mathcal{T}^c \subset \mathcal{T}_0^c$ holds with probability at least

$$1 - CsK^{3/2} \left(\frac{K^2 p_1}{e^2} \right)^{K/2},$$

where

$$p_2 = C_1 \exp \left\{ \frac{-n_{\epsilon, \delta, s, R} s^{-\omega}}{2CH\tau^2 + 2s^{-\frac{\omega}{2}}\tau} + C_2 \log(H) \right\}.$$

It can be implied that we only need

$$H \log H \ll \min(n_{\epsilon, \delta, s, R} s^{-\omega} \nu^{-2}, n_{\epsilon, \delta, s, R} H^{-1} \tau^{-2} s^{-\omega}).$$

Under this assumption, we have $\mathcal{T} = \mathcal{T}_0$ with probability converging to one. Thus we know $\mathcal{T}_0 = \mathcal{T}$ with probability converging to one, allowing us to draw some conclusions for high-dimensional FSIR.

Theorem 9. Under condition 1 - 6 and assumption 1 and choosing the same t as Theorem 8, if $H \log H \ll \min(n_{\epsilon, \delta, s, R} s^{-\omega} \nu^{-2}, n_{\epsilon, \delta, s, R} H^{-1} \tau^{-2} s^{-\omega})$, we have

$$\|e(\widehat{\Lambda}^{\mathcal{T}_0, \mathcal{T}_0}) - \Lambda\|_2 \rightarrow 0$$

as $n \rightarrow \infty$ with probability converging to one.

Theorem 10. Under the same conditions and assumptions in Theorem 9

$$\|e\left\{(\widehat{\Sigma}^{\mathcal{T}_0, \mathcal{T}_0})^{-1} \widehat{\Lambda}^{\mathcal{T}_0, \mathcal{T}_0}\right\} - e\left\{(\Sigma^{\mathcal{T}_0, \mathcal{T}_0})^{-1} \Lambda^{\mathcal{T}_0, \mathcal{T}_0}\right\}\|_2 \rightarrow 0$$

as $n \rightarrow \infty$ with probability converging to 1.

By the sparsity of β , $e\left\{(\Sigma^{\mathcal{T}, \mathcal{T}})^{-1} \Lambda^{\mathcal{T}, \mathcal{T}}\right\}$ can be regarded as the true central subspace, thus it is reasonable using $e\left\{(\widehat{\Sigma}^{\mathcal{T}_0, \mathcal{T}_0})^{-1} \widehat{\Lambda}^{\mathcal{T}_0, \mathcal{T}_0}\right\}$ as the estimation of central subspace when $\mathcal{T}_0 = \mathcal{T}$.

5 Simulation studies

5.1 Simulation setting

We consider five models in simulation studies; see details below. Among them, Model (I) uses the logistic regression to generates a binary response Y by a single index $\beta_1^T X$, where $\beta_1 \in \mathbb{R}^p$. Model (II) is another single index model emphasizing a heterogeneous covariance structure. For both of them, the structure dimension $\dim(\mathcal{S}_{Y|X}) = 1$. Model (III) and (IV) further consider the double index setting. Without loss of generality, we specify a $\beta_2 \in \mathbb{R}^p$ which is orthogonal to β_1 , so $\dim(\mathcal{S}_{Y|X}) = 2$. For each of the Model (II) to (IV), assume $\epsilon \sim N(0, 1)$ and $\epsilon \perp\!\!\!\perp X$. Model (V) presents an inverse regression model with $\epsilon \sim N(0, I_p)$ and $\epsilon \perp\!\!\!\perp Y$. Denote matrix $\Gamma \triangleq (\beta_1, \beta_2) \in \mathbb{R}^{p \times 2}$, then it is semi-orthogonal and $\mathcal{S}_{Y|X} = \text{span}(\Gamma)$; see (Cook and Forzani, 2008).

- (I) $Y = 1/\{1 + \exp(\beta_1^T X)\} > 0.5$, where $X \sim N(0, I_p)$.
- (II) $Y = \frac{1}{0.5 + (\beta_1^T X + 1)^2} + \epsilon$ where $X \sim N(0, \Sigma)$ with $\Sigma_{i,j} = 0.5^{|i-j|}$ for $1 \leq i, j \leq p$.
- (III) $Y = \frac{\beta_1^T X}{(\beta_2^T X)^3 + 1} + \epsilon$ where $X \sim N(0, I_p)$.
- (IV) $Y = \sin(\beta_1^T X) \exp(\beta_2^T X + \epsilon)$ where $X \sim N(0, \Sigma)$ with $\Sigma_{i,j} = 0.5^{|i-j|}$ for $1 \leq i, j \leq p$.
- (V) $X = \Gamma f(Y) + \epsilon$ where $\Gamma \triangleq (\beta_1, \beta_2) \in \mathbb{R}^{p \times 2}$, $f(Y) = (Y, Y^2)^T$ and $Y \sim N(0, 1)$.

In the low-dimensional setting, we take a fixed covariate dimension $p = 10$. For model (I) and (II), generate $\beta_{1,j} \sim \text{Unif}(0.4, 0.8)$ for $1 \leq j \leq p$ and set β_1 by normalizing $(\beta_{1,1}, \dots, \beta_{1,p})^T$. For model (III) to (V), specify $\beta_1 = (1, 1, 1, 1, 1, 0, \dots, 0)^T / \sqrt{5}$ and $\beta_2 = (0, 0, 0, 0, 0, 1, \dots, 1)^T / \sqrt{5}$. In the high-dimensional setting, specify $p = 500, 1000, 2000$, separately. Denote the size of active set by s and let $s_0 \triangleq \lceil s/2 \rceil$. When $p \leq 500$, we take $s = 5$, otherwise, $s = 10$. For model (I) and (II), generate $\beta_{1,j} \sim \text{Unif}(0.4, 0.8)$ for $1 \leq j \leq s$ and $\beta_{1,j} = 0$ for $s < j \leq p$. For model (III) to (V), set $\beta_{1,j} = 1$ for $1 \leq j \leq s_0$ and $\beta_{1,j} = 0$ for $s_0 < j \leq p$; similarly, set $\beta_{2,j} = 1$ for $s - s_0 \leq j \leq s$ and $\beta_{2,j} = 0$ otherwise. Finally, β_1 and β_2 are obtained by normalizing $(\beta_{1,1}, \dots, \beta_{1,p})^T$ and $(\beta_{2,1}, \dots, \beta_{2,p})^T$ respectively.

To evaluate the accuracy of the estimated $\hat{\beta}$, we use the so-called projection loss

$$d(\hat{\beta}, \beta) = \|\hat{\beta}(\hat{\beta}^\top \hat{\beta})^{-1} \hat{\beta}^\top - \beta(\beta^\top \beta)^{-1} \beta^\top\|_F,$$

which measures the distance between the subspace spanned by $\hat{\beta}$ and the target subspace spanned by β in a coordinate-free manner. The angle between $\hat{\beta}$ and β , denoted by $\angle(\hat{\beta}, \beta)$, is also utilized to present results in a more intuitive way.

5.2 Results

The first part of our study illustrates the cost of (ϵ, δ) -privacy in SIR estimation. We compare two strategies for ensuring the privacy of the slice mean matrix: the vanilla i.i.d. Gaussian mechanism and the improved multivariate Gaussian (MVG) mechanism. We denote the SIR combined with the former strategy as SIR-IID and the latter as SIR-MVG. To conduct analysis, we generate datasets for models (I), (III), and (V) separately, varying the sample size n from 100 to 50000. In each experiment, we calculate the angle $\angle(\hat{\beta}, \beta)$, where $\hat{\beta}$ is estimated using the original SIR, SIR-IID, and SIR-MVG, respectively. Figure 2 plots the averaged angle obtained from 400 replications, with an error bar locating 90% of the results. The plot clearly shows that SIR-MVG, indicated by the red curve, significantly outperforms SIR-IID, represented by the light blue curve, across all three models. Notably, SIR-IID yields unsatisfactory results for Model (III) and (V), both of which assume a structure dimension $d = 2$. Furthermore, as the sample size increases, the curve of SIR-MVG approaches the lower bound achieved by the original SIR method. This observation suggests that the multivariate Gaussian mechanism introduces only a negligible loss of accuracy when the sample size is sufficiently large.

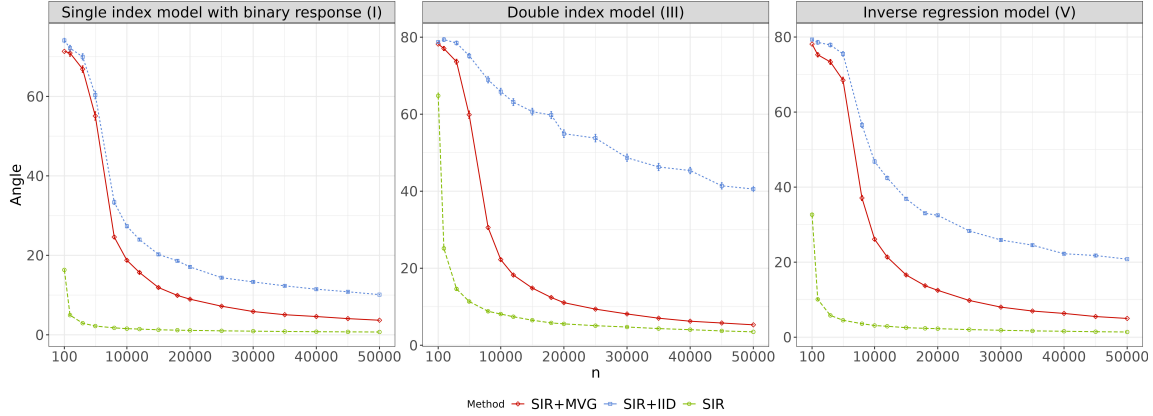


Figure 2: The cost of (ϵ, δ) -privacy in the SIR estimation.

The subsequent study investigates the effectiveness of the federated paradigm by reporting the performance of two approaches, namely FSIR-IID and FSIR-MVG, under Model (I). As mentioned earlier, Model (I) involves a binary response, which implies that the estimated $\hat{\beta}$ is scaled to the discriminant direction LDA gives. Consequently, this study also evaluates the performance of two differentially private LDA methods within the federated framework. We take the client sample size $n \in \{200, 500, 1000, 1500\}$ and the client number K ranges from 2 to 200. In each setting, we calculate $\angle(\hat{\beta}, \beta)$ and repeat the corresponding experiment 400 times. Figure 3 depicts the averaged angles for two methods against K . The results demonstrate

that both methods achieve smaller angles as K increases. Moreover, FSIR-MVG performs better than FSIR-IID across all settings, except when $n = 200$ and $\epsilon = 0.5$. This finding reveals a limitation of FSIR-MVG: when the client sample size is extremely limited, employing a highly stringent MVG mechanism on inaccurate local slice mean matrices may lead to a notable bias in estimating β , thus reducing the efficiency of the federated paradigm.

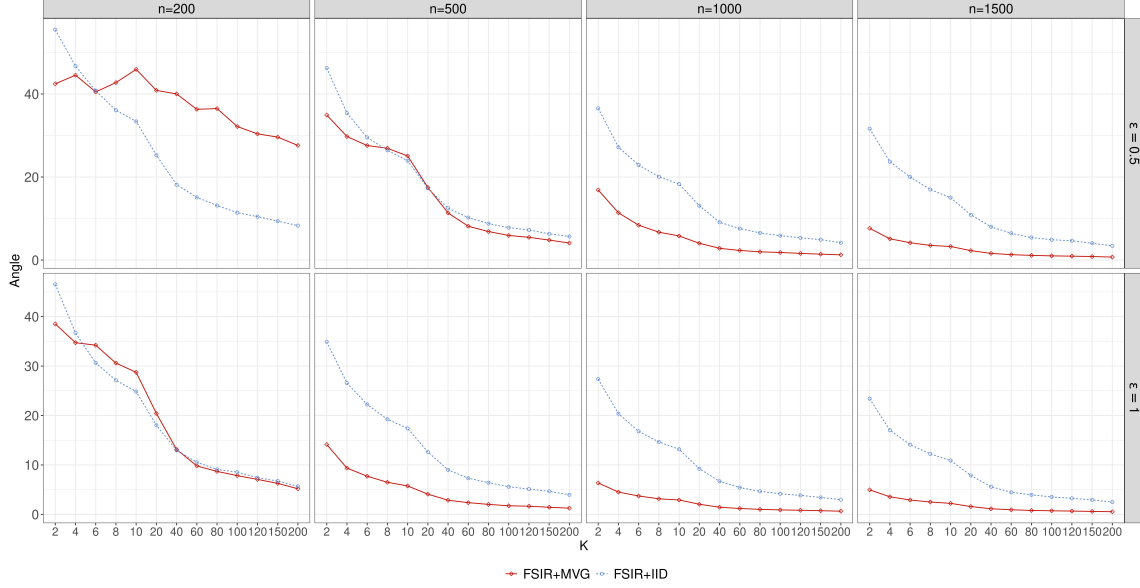
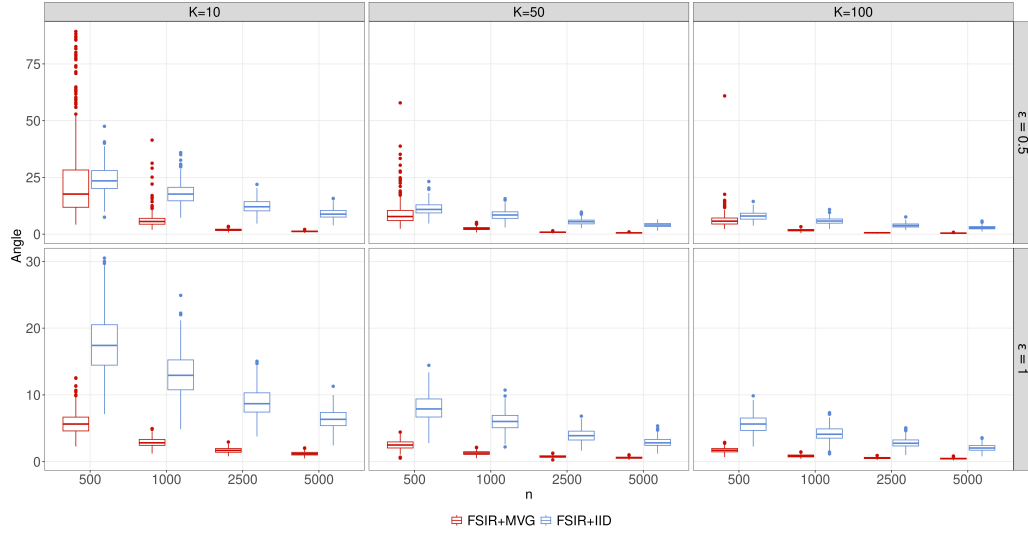


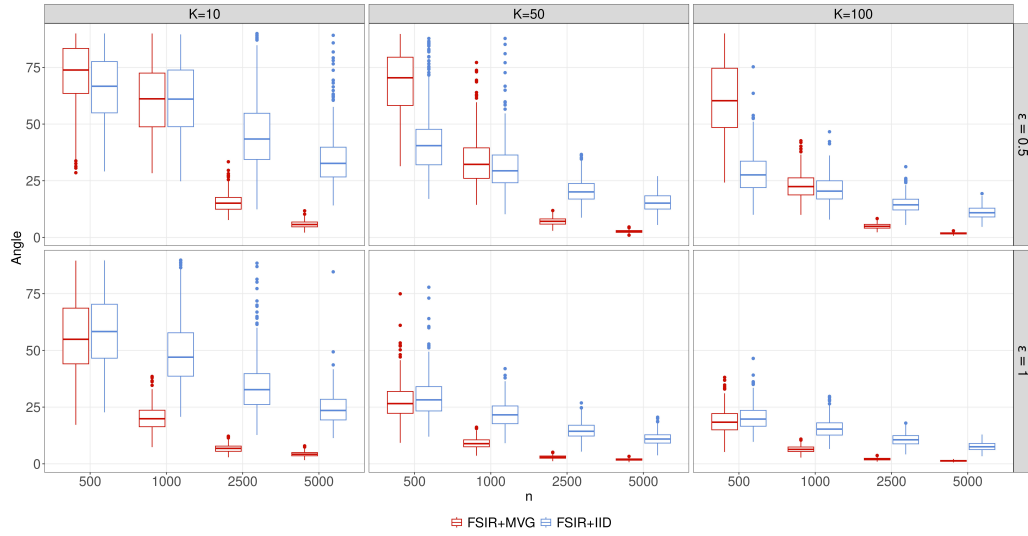
Figure 3: Averaged angle of FSIR-IID and FSIR-MVG calculated for model (I) plotted against client number K , with privacy level set (ϵ, δ) at $(0.5, 10/\lceil \frac{n}{H} \rceil^{1.1})$ and $(1, 10/\lceil \frac{n}{H} \rceil^{1.1})$ separately. From left to right, the client sample size n ranges from 200 to 1500.

Figure 4 provides a more detailed comparison between FSIR-IID and FSIR-MVG. In this analysis, Model (III) is also included to evaluate the performance of two approaches when $\dim(\mathcal{S}_{Y|X}) = 2$. We consider $K \in \{10, 50, 100\}$ and $\epsilon \in \{0.5, 1\}$. The boxplots of $\angle(\beta, \hat{\beta})$ based on 400 replicates show that FSIR-MVG outperforms FSIR-IID in most settings, except when both the sample size and the client number are limited. Particularly, FSIR-IID suffers from less accuracy under the double index model. These findings provide a valuable reference for choosing FSIR-IID or FSIR-MVG in practical applications.

For a comprehensive assessment of FSIR-IID and FSIR-MVG, we evaluate their performance across all five models using the subspace distance metric, $d(\beta, \hat{\beta})$. In the low-dimensional setting, we conduct experiments for combinations of client sample size $n \in \{500, 1000, 2500, 5000\}$ and client number $K \in \{1, 10, 50, 100\}$. Table 1 and 2 report the averaged $d(\beta, \hat{\beta})$ based on 400 replications, with standard errors in parenthesis. Notice when $K = 1$, indicating a single client in the federated framework, FSIR-IID (FSIR-MVG) reduces to SIR-IID (SIR-MVG). For high-dimensional cases, we fix $n = 1000$ for each client and set $p = 500, 1000, 2000$. The simulation results are summarized in Table 3 and 4.



(a) Model (I).



(b) Model (III).

Figure 4: Boxplots of angles calculated by FSIR-IID and FSIR-MVG over 400 repetitions as client sample size n increases from 500 to 5000. Panel (a): Model (I) with client number $K = 10, 50$ and 100 separately. The privacy level set (ϵ, δ) takes value $(0.5, 10/\lceil \frac{n}{H} \rceil^{1.1})$ in the first row of panel, and $(1, 10/\lceil \frac{n}{H} \rceil^{1.1})$ in the second row. The slices number H is fixed to 8 in each setting. Panel (b): similar to Panel (a) but under Model (III).

6 Real data analysis

6.1 Human Activity Recognition with Smartphones

To evaluate our methods on classification problem, we examine the human activity recognition dataset (Anguita et al., 2013), which can be downloaded from the UCI website. The data were collected from 30

Table 1: $p = 10$, $H = 6$, $\epsilon = 0.5$.

n	FSIR-IID				FSIR-MVG			
	K=1	K=10	K=50	K=100	K=1	K=10	K=50	K=100
I	500	1.244 (0.164)	0.574 (0.131)	0.273 (0.066)	0.197 (0.044)	1.115 (0.248)	0.545 (0.344)	0.230 (0.122)
	1000	0.950 (0.195)	0.365 (0.089)	0.171 (0.042)	0.120 (0.029)	0.357 (0.148)	0.079 (0.020)	0.035 (0.008)
	2500	0.821 (0.175)	0.301 (0.069)	0.135 (0.032)	0.096 (0.024)	0.196 (0.048)	0.047 (0.011)	0.021 (0.005)
	5000	0.622 (0.153)	0.221 (0.052)	0.099 (0.023)	0.071 (0.018)	0.108 (0.026)	0.031 (0.007)	0.015 (0.004)
II	500	1.406 (0.011)	1.360 (0.054)	1.177 (0.122)	1.044 (0.146)	1.381 (0.063)	1.321 (0.087)	1.282 (0.114)
	1000	1.402 (0.019)	1.285 (0.086)	0.982 (0.160)	0.811 (0.160)	1.290 (0.122)	1.071 (0.182)	0.730 (0.161)
	2500	1.394 (0.029)	1.218 (0.109)	0.860 (0.163)	0.702 (0.151)	1.160 (0.155)	0.699 (0.169)	0.361 (0.100)
	5000	1.373 (0.056)	1.112 (0.136)	0.729 (0.155)	0.564 (0.146)	0.759 (0.172)	0.295 (0.074)	0.158 (0.035)
III	500	1.755 (0.129)	1.439 (0.160)	0.986 (0.210)	0.718 (0.178)	1.638 (0.160)	1.498 (0.175)	1.412 (0.169)
	1000	1.678 (0.156)	1.206 (0.214)	0.670 (0.152)	0.474 (0.106)	1.418 (0.158)	0.904 (0.213)	0.423 (0.090)
	2500	1.627 (0.147)	1.061 (0.222)	0.529 (0.114)	0.380 (0.086)	1.134 (0.227)	0.398 (0.089)	0.183 (0.040)
	5000	1.514 (0.163)	0.840 (0.207)	0.398 (0.091)	0.287 (0.061)	0.471 (0.106)	0.151 (0.035)	0.069 (0.015)
IV	500	1.929 (0.068)	1.526 (0.143)	0.990 (0.152)	0.779 (0.126)	1.797 (0.136)	1.543 (0.178)	1.417 (0.178)
	1000	1.837 (0.095)	1.236 (0.158)	0.710 (0.123)	0.541 (0.099)	1.456 (0.192)	0.867 (0.157)	0.452 (0.099)
	2500	1.758 (0.107)	1.076 (0.161)	0.591 (0.110)	0.448 (0.089)	1.080 (0.186)	0.426 (0.087)	0.247 (0.037)
	5000	1.619 (0.131)	0.873 (0.148)	0.460 (0.089)	0.349 (0.060)	0.498 (0.097)	0.218 (0.028)	0.174 (0.012)
V	500	1.877 (0.086)	1.296 (0.139)	0.750 (0.117)	0.554 (0.090)	1.566 (0.182)	1.318 (0.202)	1.208 (0.219)
	1000	1.713 (0.126)	0.979 (0.134)	0.505 (0.093)	0.360 (0.065)	1.133 (0.203)	0.728 (0.189)	0.379 (0.079)
	2500	1.615 (0.133)	0.835 (0.134)	0.409 (0.080)	0.290 (0.050)	0.864 (0.211)	0.349 (0.078)	0.162 (0.032)
	5000	1.414 (0.145)	0.637 (0.108)	0.308 (0.058)	0.217 (0.040)	0.387 (0.080)	0.126 (0.025)	0.056 (0.011)

Table 2: $p = 10$, $H = 6$, $\epsilon = 1$.

n	FSIR-IID				FSIR-MVG			
	K=1	K=10	K=50	K=100	K=1	K=10	K=50	K=100
I	500	1.026 (0.200)	0.427 (0.102)	0.197 (0.048)	0.139 (0.033)	0.612 (0.263)	0.143 (0.040)	0.062 (0.016)
	1000	0.760 (0.180)	0.269 (0.064)	0.122 (0.029)	0.085 (0.020)	0.183 (0.046)	0.054 (0.013)	0.024 (0.006)
	2500	0.617 (0.142)	0.218 (0.052)	0.096 (0.023)	0.070 (0.017)	0.130 (0.029)	0.042 (0.010)	0.019 (0.004)
	5000	0.476 (0.117)	0.157 (0.037)	0.071 (0.017)	0.051 (0.012)	0.084 (0.020)	0.030 (0.007)	0.014 (0.003)
II	500	1.404 (0.018)	1.306 (0.075)	1.043 (0.150)	0.861 (0.160)	1.362 (0.067)	1.228 (0.129)	0.961 (0.170)
	1000	1.387 (0.033)	1.183 (0.123)	0.823 (0.164)	0.638 (0.144)	1.111 (0.157)	0.536 (0.136)	0.277 (0.071)
	2500	1.378 (0.040)	1.095 (0.146)	0.697 (0.151)	0.537 (0.136)	0.810 (0.162)	0.317 (0.081)	0.166 (0.039)
	5000	1.338 (0.063)	0.968 (0.149)	0.552 (0.140)	0.420 (0.113)	0.532 (0.127)	0.201 (0.049)	0.122 (0.024)
III	500	1.694 (0.150)	1.284 (0.193)	0.734 (0.171)	0.524 (0.121)	1.522 (0.164)	1.221 (0.207)	0.688 (0.163)
	1000	1.586 (0.156)	0.995 (0.220)	0.488 (0.112)	0.334 (0.071)	0.907 (0.206)	0.301 (0.063)	0.133 (0.030)
	2500	1.492 (0.172)	0.833 (0.202)	0.381 (0.079)	0.276 (0.060)	0.538 (0.114)	0.178 (0.040)	0.078 (0.017)
	5000	1.385 (0.170)	0.617 (0.144)	0.287 (0.065)	0.201 (0.045)	0.344 (0.074)	0.112 (0.025)	0.050 (0.010)
IV	500	1.888 (0.078)	1.314 (0.153)	0.774 (0.143)	0.574 (0.108)	1.682 (0.157)	1.155 (0.188)	0.685 (0.120)
	1000	1.713 (0.123)	1.000 (0.148)	0.533 (0.099)	0.401 (0.078)	0.859 (0.153)	0.330 (0.057)	0.208 (0.025)
	2500	1.598 (0.130)	0.853 (0.140)	0.446 (0.086)	0.340 (0.061)	0.517 (0.094)	0.227 (0.032)	0.178 (0.013)
	5000	1.409 (0.155)	0.672 (0.112)	0.349 (0.063)	0.273 (0.043)	0.322 (0.056)	0.187 (0.019)	0.168 (0.009)
V	500	1.773 (0.114)	1.065 (0.137)	0.561 (0.100)	0.399 (0.079)	1.383 (0.204)	1.033 (0.206)	0.601 (0.129)
	1000	1.540 (0.131)	0.761 (0.114)	0.366 (0.069)	0.261 (0.047)	0.735 (0.157)	0.255 (0.053)	0.112 (0.022)
	2500	1.399 (0.147)	0.626 (0.102)	0.296 (0.054)	0.209 (0.037)	0.427 (0.080)	0.139 (0.027)	0.061 (0.012)
	5000	1.173 (0.150)	0.476 (0.089)	0.220 (0.040)	0.154 (0.030)	0.246 (0.050)	0.082 (0.015)	0.036 (0.007)

Table 3: $n = 1000$, $H = 8$, $\epsilon = 0.5$.

p	FSIR-IID				FSIR-MVG			
	K=1	K=10	K=50	K=100	K=1	K=10	K=50	K=100
I	500	0.685 (0.228)	0.225 (0.077)	0.100 (0.036)	0.072 (0.024)	0.174 (0.066)	0.050 (0.018)	0.026 (0.010)
	1000	1.028 (0.204)	0.385 (0.090)	0.180 (0.044)	0.127 (0.029)	0.619 (0.278)	0.129 (0.040)	0.057 (0.015)
	2000	1.060 (0.195)	0.387 (0.096)	0.182 (0.046)	0.128 (0.026)	0.606 (0.260)	0.132 (0.043)	0.057 (0.015)
II	500	1.405 (0.014)	0.907 (0.238)	0.520 (0.164)	0.415 (0.132)	1.389 (0.033)	0.800 (0.250)	0.488 (0.153)
	1000	1.403 (0.013)	1.225 (0.114)	0.865 (0.169)	0.674 (0.161)	1.399 (0.020)	1.193 (0.155)	1.089 (0.174)
	2000	1.405 (0.013)	1.208 (0.112)	0.852 (0.151)	0.652 (0.156)	1.398 (0.024)	1.159 (0.150)	1.042 (0.184)
III	500	1.914 (0.059)	0.495 (0.179)	0.223 (0.068)	0.152 (0.046)	1.902 (0.065)	0.362 (0.141)	0.172 (0.062)
	1000	1.963 (0.028)	0.976 (0.205)	0.438 (0.082)	0.335 (0.073)	1.960 (0.028)	1.260 (0.208)	0.817 (0.183)
	2000	1.962 (0.030)	0.978 (0.219)	0.499 (0.090)	0.397 (0.091)	1.959 (0.029)	1.250 (0.217)	0.794 (0.177)
IV	500	1.941 (0.042)	0.875 (0.186)	0.474 (0.110)	0.352 (0.091)	1.898 (0.064)	0.817 (0.189)	0.519 (0.146)
	1000	1.963 (0.025)	1.322 (0.150)	0.793 (0.123)	0.599 (0.093)	1.951 (0.032)	1.394 (0.175)	1.178 (0.185)
	2000	1.967 (0.023)	1.318 (0.146)	0.757 (0.115)	0.610 (0.101)	1.958 (0.027)	1.383 (0.162)	1.179 (0.168)
V	500	1.973 (0.023)	0.572 (0.160)	0.359 (0.138)	0.309 (0.118)	1.931 (0.047)	0.591 (0.197)	0.376 (0.124)
	1000	1.967 (0.024)	0.947 (0.134)	0.539 (0.109)	0.450 (0.093)	1.958 (0.027)	1.083 (0.169)	0.842 (0.156)
	2000	1.969 (0.020)	0.932 (0.140)	0.535 (0.096)	0.459 (0.097)	1.960 (0.026)	1.051 (0.186)	0.883 (0.156)

Table 4: $n = 1000$, $H = 8$, $\epsilon = 1$.

P	FSIR-IID				FSIR-MVG			
	K=1	K=10	K=50	K=100	K=1	K=10	K=50	K=100
I	500	0.530 (0.183)	0.160 (0.058)	0.074 (0.026)	0.051 (0.019)	0.111 (0.042)	0.044 (0.016)	0.025 (0.008)
	1000	0.895 (0.190)	0.290 (0.072)	0.129 (0.030)	0.093 (0.021)	0.276 (0.079)	0.073 (0.016)	0.032 (0.007)
	2000	0.879 (0.175)	0.284 (0.072)	0.133 (0.032)	0.091 (0.022)	0.272 (0.069)	0.076 (0.018)	0.034 (0.007)
II	500	1.403 (0.014)	0.743 (0.189)	0.403 (0.129)	0.320 (0.095)	1.385 (0.041)	0.377 (0.121)	0.223 (0.056)
	1000	1.408 (0.008)	1.074 (0.149)	0.696 (0.149)	0.536 (0.141)	1.402 (0.017)	0.904 (0.178)	0.536 (0.144)
	2000	1.408 (0.009)	1.075 (0.139)	0.651 (0.147)	0.503 (0.130)	1.403 (0.016)	0.858 (0.159)	0.507 (0.134)
III	500	1.881 (0.073)	0.340 (0.113)	0.155 (0.050)	0.123 (0.042)	1.772 (0.100)	0.132 (0.047)	0.083 (0.028)
	1000	1.956 (0.031)	0.718 (0.151)	0.331 (0.075)	0.240 (0.062)	1.957 (0.026)	0.528 (0.111)	0.240 (0.061)
	2000	1.963 (0.025)	0.739 (0.127)	0.393 (0.100)	0.322 (0.110)	1.967 (0.022)	0.537 (0.089)	0.331 (0.109)
IV	500	1.920 (0.058)	0.672 (0.148)	0.351 (0.087)	0.289 (0.071)	1.834 (0.099)	0.361 (0.097)	0.234 (0.060)
	1000	1.977 (0.016)	1.077 (0.158)	0.610 (0.100)	0.452 (0.081)	1.961 (0.029)	0.926 (0.175)	0.532 (0.095)
	2000	1.975 (0.017)	1.052 (0.149)	0.600 (0.091)	0.456 (0.080)	1.960 (0.025)	0.902 (0.161)	0.519 (0.100)
V	500	1.964 (0.028)	0.475 (0.128)	0.328 (0.126)	0.310 (0.133)	1.856 (0.075)	0.323 (0.125)	0.286 (0.130)
	1000	1.981 (0.014)	0.755 (0.104)	0.455 (0.097)	0.393 (0.085)	1.966 (0.023)	0.643 (0.123)	0.415 (0.089)
	2000	1.982 (0.013)	0.725 (0.123)	0.468 (0.094)	0.411 (0.083)	1.966 (0.022)	0.630 (0.111)	0.436 (0.088)

volunteers who performed six activities (walking, walking upstairs, walking downstairs, sitting, standing, and laying) while wearing a smartphone on their waist. Sensor records were then captured using the smartphone’s embedded accelerometer and gyroscope at a rate of 50 Hz, resulting in a dataset with 10299 samples and 561 features. Given the sensitivity of cellphone data in real life, we suggest to partition the dataset into 30 disjoint subsets according to different subjects (regarded as clients), each containing no more than 410 samples, thus representing a high-dimensional setting on any single client.

In this experiment, we study three physical activity levels of a person: active (includes walking and walking downstairs/upstairs), sedentary (includes standing and sitting), and lying down. We perform FSIR and its differentially private counterparts on the decentralized dataset. With the estimated sparsity parameter $\hat{s} = 5$ and structure dimension $\hat{d} = 2$, FSIR selects 10 active covariates to construct a 2-dimensional SDR subspace $\hat{\mathcal{S}}_{Y|X}$. Figure 5 depicts 200 randomly selected samples for each activity on the estimated $\hat{\mathcal{S}}_{Y|X}$. The three activity levels are easily distinguished in each plot, demonstrating the effectiveness of our proposed methods. Notably, both FSIR-IID and FSIR-MVG guarantee a $(0.1, 1/n)$ -level differential privacy, where n is the minimum sample size of a particular activity performed by a single individual across all activities of all subjects. Due to limited sample size on clients, FSIR-MVG performs slightly worse than FSIR-IID.

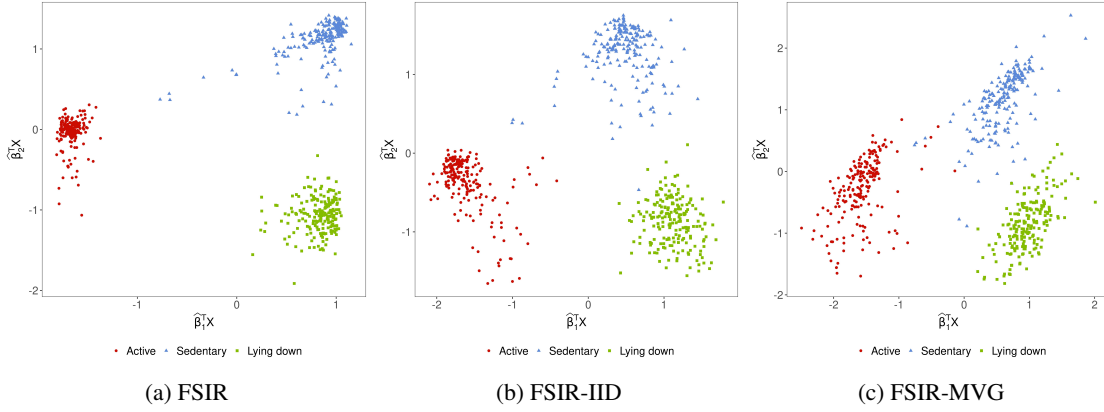


Figure 5: The scatterplot of the SDR subspace from FSIR, FSIR-IID and FSIR-MVG on a demo subset of the human activity recognition dataset.

6.2 Airline on-time performance

We apply our method to an airline on-time performance data in the R package “nycflights13”. This dataset comprises information on 336,776 flights that departed from various airports in NYC (e.g., EWR, JFK, and LGA) to different destinations in year 2013. Our object is to analyze the Arrival delay based on seven variables: Month, Day, Departure Delay, Arrival time, Scheduled arrival time, Air time, and Distance. We divide the dataset into disjoint clients according to 11 selected airlines, each containing $n = 5000$ samples. We set the privacy level set to $(\epsilon, \delta) = (0.1, 1/n)$, ensuring a satisfactory level of privacy protection for the clients’ data. Figure 6 illustrates the estimated $\hat{S}Y|X$ based on a randomly selected subset of 2000 samples. We can see when an adequate number of samples is available, FSIR-MVG is preferable.

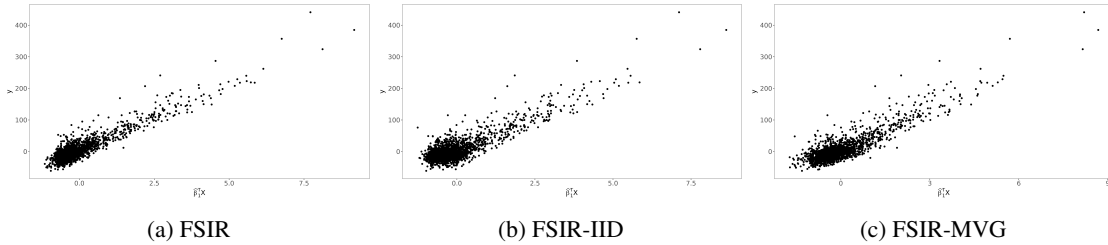


Figure 6: The scatterplot of the central subspace from FSIR, FSIR-IID and FSIR-MVG on a demo subset of airline dataset.

7 Discussion

We provide a federated framework for performing sufficient dimension reduction on decentralized data, ensuring both data ownership and privacy. As the first investigation on privacy protection of the SDR subspace estimation, we clarify our idea in a relative simple setting, which implicitly assumes that data on different clients are homogeneous. In practice, however, data might not be identically distributed across clients and we leave this heterogeneous scenario for future study. Considering the SIR estimator still suffers from some limitations, we claim that strategies and technical tools provided in the work can help many other SDR estimators develop their own federated extensions, with a differentially private guarantee.

References

- Martin Abadi, Andy Chu, Ian Goodfellow, H Brendan McMahan, Ilya Mironov, Kunal Talwar, and Li Zhang. Deep learning with differential privacy. In *Proceedings of the 2016 ACM SIGSAC conference on computer and communications security*, pages 308–318, 2016.
- Davide Anguita, Alessandro Ghio, Luca Oneto, Xavier Parra, Jorge Luis Reyes-Ortiz, et al. A public domain dataset for human activity recognition using smartphones. In *Esann*, volume 3, page 3, 2013.
- D Apple. Learning with privacy at scale. *Apple Machine Learning Journal*, 1(8), 2017.
- Marco Avella-Medina. Privacy-preserving parametric inference: a case for robust statistics. *Journal of the American Statistical Association*, 116(534):969–983, 2021.

- Raef Bassily, Adam Smith, and Abhradeep Thakurta. Private empirical risk minimization: Efficient algorithms and tight error bounds. In *2014 IEEE 55th annual symposium on foundations of computer science*, pages 464–473. IEEE, 2014.
- Sourav Biswas, Yihe Dong, Gautam Kamath, and Jonathan Ullman. Coinpress: Practical private mean and covariance estimation. *Advances in Neural Information Processing Systems*, 33:14475–14485, 2020.
- Mark Bun, Jonathan Ullman, and Salil Vadhan. Fingerprinting codes and the price of approximate differential privacy. In *Proceedings of the forty-sixth annual ACM symposium on Theory of computing*, pages 1–10, 2014.
- Efstathia Bura and R Dennis Cook. Extending sliced inverse regression: The weighted chi-squared test. *Journal of the American Statistical Association*, 96(455):996–1003, 2001.
- T Tony Cai, Yichen Wang, and Linjun Zhang. The cost of privacy: Optimal rates of convergence for parameter estimation with differential privacy. *The Annals of Statistics*, 49(5):2825–2850, 2021.
- Zhanrui Cai, Runze Li, and Liping Zhu. Online sufficient dimension reduction through sliced inverse regression. *The Journal of Machine Learning Research*, 21(1):321–345, 2020.
- Joseph A Calandrino, Ann Kilzer, Arvind Narayanan, Edward W Felten, and Vitaly Shmatikov. ” you might also like:” privacy risks of collaborative filtering. In *2011 IEEE symposium on security and privacy*, pages 231–246. IEEE, 2011.
- Kamalika Chaudhuri, Anand Sarwate, and Kaushik Sinha. Near-optimal differentially private principal components. *Advances in neural information processing systems*, 25, 2012.
- Kamalika Chaudhuri, Anand D Sarwate, and Kaushik Sinha. A near-optimal algorithm for differentially-private principal components. *Journal of Machine Learning Research*, 14, 2013.
- Canyi Chen, Wangli Xu, and Liping Zhu. Distributed estimation in heterogeneous reduced rank regression: With application to order determination in sufficient dimension reduction. *Journal of Multivariate Analysis*, 190:104991, 2022.
- Chun-Houh Chen and Ker-Chau Li. Generalization of fisher’ s linear discriminant analysis via the approach of sliced inverse regression. *Journal of the Korean Statistical Society*, 30(2):193–217, 2001.
- Xin Chen, Changliang Zou, and R Dennis Cook. Coordinate-independent sparse sufficient dimension reduction and variable selection. 2010.
- R Dennis Cook. On the interpretation of regression plots. *Journal of the American Statistical Association*, 89(425):177–189, 1994.
- R Dennis Cook. Graphics for regressions with a binary response. *Journal of the American Statistical Association*, 91(435):983–992, 1996.
- R Dennis Cook. *Regression graphics: Ideas for studying regressions through graphics*. John Wiley & Sons, 2009.
- R Dennis Cook and Liliana Forzani. Principal fitted components for dimension reduction in regression. *Statistical Science*, 23(4):485–501, 2008.

- Wenquan Cui, Yue Zhao, Jianjun Xu, and Haoyang Cheng. Federated sufficient dimension reduction through high-dimensional sparse sliced inverse regression. *arXiv preprint arXiv:2301.09500*, 2023.
- Bolin Ding, Janardhan Kulkarni, and Sergey Yekhanin. Collecting telemetry data privately. *Advances in Neural Information Processing Systems*, 30, 2017.
- Jörg Drechsler. Differential privacy for government agencies—are we there yet? *Journal of the American Statistical Association*, (just-accepted):1–24, 2022.
- Jörg Drechsler. Differential privacy for government agencies—are we there yet? *Journal of the American Statistical Association*, 118(541):761–773, 2023.
- Rui Duan, Yang Ning, and Yong Chen. Heterogeneity-aware and communication-efficient distributed statistical inference. *Biometrika*, 109(1):67–83, 2022.
- Cynthia Dwork and Jing Lei. Differential privacy and robust statistics. In *Proceedings of the forty-first annual ACM symposium on Theory of computing*, pages 371–380, 2009.
- Cynthia Dwork, Frank McSherry, Kobbi Nissim, and Adam Smith. Calibrating noise to sensitivity in private data analysis. In *Theory of cryptography conference*, pages 265–284. Springer, 2006.
- Cynthia Dwork, Aaron Roth, et al. The algorithmic foundations of differential privacy. *Foundations and Trends® in Theoretical Computer Science*, 9(3–4):211–407, 2014.
- Cynthia Dwork, Adam Smith, Thomas Steinke, Jonathan Ullman, and Salil Vadhan. Robust traceability from trace amounts. In *2015 IEEE 56th Annual Symposium on Foundations of Computer Science*, pages 650–669. IEEE, 2015.
- Cynthia Dwork, Adam Smith, Thomas Steinke, and Jonathan Ullman. Exposed! a survey of attacks on private data. *Annu. Rev. Stat. Appl.*, 4(1):61–84, 2017.
- Cynthia Dwork, Weijie J Su, and Li Zhang. Differentially private false discovery rate control. *arXiv preprint arXiv:1807.04209*, 2018.
- Úlfar Erlingsson, Vasyl Pihur, and Aleksandra Korolova. Rappor: Randomized aggregatable privacy-preserving ordinal response. In *Proceedings of the 2014 ACM SIGSAC conference on computer and communications security*, pages 1054–1067, 2014.
- Andreas Grammenos, Rodrigo Mendoza Smith, Jon Crowcroft, and Cecilia Mascolo. Federated principal component analysis. *Advances in Neural Information Processing Systems*, 33:6453–6464, 2020.
- Nils Homer, Szabolcs Szelinger, Margot Redman, David Duggan, Waibhav Tembe, Jill Muehling, John V Pearson, Dietrich A Stephan, Stanley F Nelson, and David W Craig. Resolving individuals contributing trace amounts of dna to highly complex mixtures using high-density snp genotyping microarrays. *PLoS genetics*, 4(8):e1000167, 2008.
- Wuxuan Jiang, Cong Xie, and Zhihua Zhang. Wishart mechanism for differentially private principal components analysis. In *Proceedings of the AAAI Conference on Artificial Intelligence*, volume 30, 2016.
- Gautam Kamath, Jerry Li, Vikrant Singhal, and Jonathan Ullman. Privately learning high-dimensional distributions. In *Conference on Learning Theory*, pages 1853–1902. PMLR, 2019.

- Jing Lei. Differentially private m-estimators. *Advances in Neural Information Processing Systems*, 24, 2011.
- Ker-Chau Li. Sliced inverse regression for dimension reduction. *Journal of the American Statistical Association*, 86(414):316–327, 1991.
- Lexin Li. Sparse sufficient dimension reduction. *Biometrika*, 94(3):603–613, 2007.
- Tian Li, Anit Kumar Sahu, Ameet Talwalkar, and Virginia Smith. Federated learning: Challenges, methods, and future directions. *IEEE signal processing magazine*, 37(3):50–60, 2020.
- Qian Lin, Zhigen Zhao, and Jun S Liu. On consistency and sparsity for sliced inverse regression in high dimensions. *The Annals of Statistics*, 46(2):580–610, 2018.
- Qian Lin, Zhigen Zhao, and Jun S Liu. Sparse sliced inverse regression via lasso. *Journal of the American Statistical Association*, 114(528):1726–1739, 2019.
- Qian Lin, Xinran Li, Dongming Huang, and Jun S. Liu. On the optimality of sliced inverse regression in high dimensions. *The Annals of Statistics*, 49(1):1 – 20, 2021. doi: 10.1214/19-AOS1813. URL <https://doi.org/10.1214/19-AOS1813>.
- Xiaokang Liu, Rui Duan, Chongliang Luo, Alexis Ogdie, Jason H Moore, Henry R Kranzler, Jiang Bian, and Yong Chen. Multisite learning of high-dimensional heterogeneous data with applications to opioid use disorder study of 15,000 patients across 5 clinical sites. *Scientific reports*, 12(1):11073, 2022.
- Wei Luo and Bing Li. On order determination by predictor augmentation. *Biometrika*, 108(3):557–574, 2021.
- Brendan McMahan, Eider Moore, Daniel Ramage, Seth Hampson, and Blaise Aguera y Arcas. Communication-efficient learning of deep networks from decentralized data. In *Artificial intelligence and statistics*, pages 1273–1282. PMLR, 2017.
- Keith W Penrose, AG Nelson, and AG Fisher. Generalized body composition prediction equation for men using simple measurement techniques. *Medicine & Science in Sports & Exercise*, 17(2):189, 1985.
- Kunal Talwar, Abhradeep Guha Thakurta, and Li Zhang. Nearly optimal private lasso. *Advances in Neural Information Processing Systems*, 28, 2015.
- Kai Tan, Lei Shi, and Zhou Yu. Sparse SIR: Optimal rates and adaptive estimation. *The Annals of Statistics*, 48(1):64 – 85, 2020. doi: 10.1214/18-AOS1791. URL <https://doi.org/10.1214/18-AOS1791>.
- Kean Ming Tan, Zhaoran Wang, Tong Zhang, Han Liu, and R Dennis Cook. A convex formulation for high-dimensional sparse sliced inverse regression. *Biometrika*, 105(4):769–782, 2018.
- Jiayi Tong, Chongliang Luo, Md Nazmul Islam, Natalie E Sheils, John Buresh, Mackenzie Edmondson, Peter A Merkel, Ebbing Lautenbach, Rui Duan, and Yong Chen. Distributed learning for heterogeneous clinical data with application to integrating covid-19 data across 230 sites. *NPJ digital medicine*, 5(1):76, 2022.
- R Vershynin. Introduction to the non-asymptotic analysis of random matrices. In *Compress Sensing*, pages 210–268. Cambridge Univ Press, 2012.

- Di Wang and Jinhui Xu. Differentially private high dimensional sparse covariance matrix estimation. *Theoretical Computer Science*, 865:119–130, 2021.
- Larry Wasserman and Shuheng Zhou. A statistical framework for differential privacy. *Journal of the American Statistical Association*, 105(489):375–389, 2010.
- H Weyl. "das asymptotische verteilungsgesetz der eigenwerte linearer partieller differentialgleichungen". *Math. Ann*, 71:441–479, 1912.
- Kelin Xu, Liping Zhu, and Jianqing Fan. Distributed sufficient dimension reduction for heterogeneous massive data. *Statistica Sinica*, 32:2455–2476, 2022.
- Jing Zeng, Qing Mai, and Xin Zhang. Subspace estimation with automatic dimension and variable selection in sufficient dimension reduction. *Journal of the American Statistical Association*, pages 1–13, 2022.